The Astrophysical Journal, 719:685–690, 2010 August 10 doi:10.1088/0004-637X/719/1/685

NEW RESULTS FROM THE MAGELLAN IMACS SPECTROSCOPIC Lyα SURVEY: NICMOS OBSERVATIONS OF Lyα EMITTERS AT $z = 5.7$*

Alaina L. Henry[1], Crystal L. Martin[1], Alan Dressler[2], Patrick McCarthy[2], and Marcin Sawicki[3]
[1] Department of Physics, University of California, Santa Barbara, CA 93106, USA; ahenry@physics.ucsb.edu
[2] Observatories of the Carnegie Institute of Washington, Santa Barbara Street, Pasadena, CA 91101, USA
[3] Department of Astronomy and Physics, Saint Mary's University, Halifax, NS B3H 3C3, Canada
Received 2010 April 26; accepted 2010 June 14; published 2010 July 22

ABSTRACT

We present NICMOS J_{110} (rest-frame 1200–2100 Å) observations of the three $z = 5.7$ Lyα emitters discovered in the blind multislit spectroscopic survey by Martin et al. These images confirm the presence of the two sources that were previously only seen in spectroscopic observations. The third source, which is undetected in our J_{110} observations, has been detected in narrowband imaging of the Cosmic Origins Survey, so our non-detection implies a rest-frame equivalent width >146 Å (3σ). The two J_{110}-detected sources have more modest rest-frame equivalent widths of 30–40 Å, but all three are typical of high-redshift Lyα emitters. In addition, the J_{110}-detected sources have UV luminosities that are within a factor of 2 of $L^*_{\rm UV}$, and sizes that appear compact ($r_{\rm hl} \sim 0\farcs15$) in our NIC2 images—consistent with a redshift of 5.7. We use these UV-continuum and Lyα measurements to estimate the $i_{775}-z_{850}$ colors of these galaxies and show that at least one and possibly all three would be missed by the *i*-dropout Lyman break galaxy selection. These observations help demonstrate the utility of multislit narrowband spectroscopy as a technique for finding faint emission-line galaxies.

Key words: galaxies: evolution – galaxies: formation – galaxies: high-redshift

1. INTRODUCTION

Studying the epoch around $z \sim 6$ is important for our understanding of the early stages of galaxy formation. It is around this time, when the age of the universe was less than a Gyr, that the reionization of the hydrogen component of the intergalactic medium (IGM) was substantially completed (Fan et al. 2006). Hundreds of $z \sim 6$ galaxies have now been photometrically selected (e.g., Bouwens et al. 2007; McLure et al. 2009), and at least tens of Lyman break galaxies (LBGs) and many more Lyα emitters (LAEs) are now spectroscopically confirmed (Dow-Hygelund et al. 2007; Vanzella et al. 2009; Stanway et al. 2007; Kashikawa et al. 2006; Shimasaku et al. 2006; Stark et al. 2010). While there are hints of substantial star formation at even higher redshifts (Eyles et al. 2005, 2007; Yan et al. 2006; Simcoe 2006; Ryan-Weber et al. 2009; Dunkley et al. 2009; Bouwens et al. 2008, 2010; Bunker et al. 2009), $z \sim 6$ remains the earliest epoch for which robust galaxy samples are available.

At $z \sim 6$, galaxies are selected via the Lyman break method (Meier 1976; Steidel et al. 1996) or because of strong Lyα emission (Hu et al. 2002, 2004; Rhoads et al. 2004; Ajiki et al. 2004; Westra et al. 2006). Both methods select star-forming galaxies, but the two populations differ. Not all LBGs have Lyα emission (Shapley et al. 2003; Stanway et al. 2007; Vanzella et al. 2009) and LAEs can be missed by LBG surveys because they are faint in the continuum or their Lyα emission contaminates broadband photometry. Studies of LAEs are an important complement to LBG surveys, because the faint continuum luminosities and high specific star formation rates (SFRs) of LAEs make them likely candidates for galaxy building blocks.

To date, narrowband imaging surveys have been very successful in finding LAEs at $z \sim 3$–6. Multiwavelength observations have shown that these LAEs are typically (but not always) younger and less massive, and they have lower dust extinction than LBGs (Finkelstein et al. 2007, 2008, 2009; Gawiser et al. 2006, 2007; Nilsson et al. 2007; Lai et al. 2008; Kornei et al. 2010). In addition, Lyα luminosity functions (LFs) measured at $z \sim 3$–6 show little or no evolution with redshift (Shimasaku et al. 2006; Gronwall et al. 2007; Dawson et al. 2007; Murayama et al. 2007; Ouchi et al. 2008). At higher redshifts, measurements of the Lyα LF may allow a determination of the neutral hydrogen fraction in the IGM and LAE clustering could help constrain models of the patchiness of the reionization process (Santos 2004; Santos et al. 2004; Haiman & Cen 2005; Furlanetto et al. 2006; Dijkstra et al. 2007; McQuinn et al. 2007). In fact, Kashikawa et al. (2006) now report a measured decline in the Lyα LF at $z = 6.5$, although this is not seen in a compilation of different data sets presented by Malhotra & Rhoads (2004).

Spectroscopic searches for LAEs have the potential to detect objects with fainter line emission than purely narrowband imaging, because they sample with a resolution closer to the intrinsic width of the emission line. This is especially important at $z \gtrsim 6$, where observing the faint end of the galaxy LF is challenging. However, the task is challenging and first efforts at blank sky surveys using multislit narrowband spectroscopy at Keck Observatory and the Very Large Telescope (VLT) found only low- and intermediate-redshift interlopers (Tran et al. 2004; Martin & Sawicki 2004). More recently, different spectroscopic strategies have met success. Sawicki et al. (2008) have found several faint serendipitous LAEs at $z = 4.4$–4.9 in a search of 20% of the DEEP2 database. While the area subtended by DEEP2 slits is only 21.6 arcmin^2, a large line-of-sight volume is sampled within the relatively OH-free portion of the sky spectrum at $\lambda < 7000$ Å. In addition, Rauch et al. (2008) found 27 $z \sim 3$ LAEs in a single longslit spectrum; their ∼100 hr VLT observation reached a flux 1–2 orders of

* This work is based in part on observations made with the NASA/ESA *Hubble Space Telescope*, obtained from the Space Telescope Science Institute, which is operated by the Association of Universities for Research in Astronomy Inc., under NASA contract NAS 5-26555. These observations are associated with proposal 11183.

magnitude deeper than most other LAE searches. At higher redshifts, slitless spectroscopy with the *Hubble Space Telescope* (*HST*) has uncovered a few sources at $z > 5$ (Pirzkal et al. 2007), and longslit spectroscopy of the critical lines of strong gravitational lenses has discovered low-luminosity LAEs at $z \sim 6$ (Santos et al. 2004), as well as a few candidates at $z > 8$ (Stark et al. 2007).

Recently, wider areas have become accessible with multislit narrowband spectroscopy, and LAEs have been found at $z \approx 5.7$. Using the Inamori Magellan Areal Camera and Spectrograph (IMACS; Dressler et al. 2006), Martin et al. (2008) carried out a blind spectroscopic search in 200 arcmin^2 in the Cosmic Evolution Survey (COSMOS; Scoville et al. 2007) and the 15 hr field of the Las Campanas Infrared Survey (LCIRS; Marzke et al. 1999). These observations reach a sensitivity fainter than L^*(Lyα) at $z \approx 5.7$ ($\sim$several $\times 10^{42}$ erg s^{-1}, as measured by Shimasaku et al. 2006; Ouchi et al. 2008), and three LAE candidates at $z \approx 5.7$ were confirmed with further spectroscopy. Following this success, we have carried out a deeper survey in the same fields (A. Dressler et al. 2010, in preparation), uncovering at least several sources at luminosities that were previously only reached with searches making use of strong lensing (Santos et al. 2004).

Of the three sources found by Martin et al. (2008), none are detected in the available continuum imaging, and only one has been previously detected in COSMOS narrowband imaging (no narrowband imaging is available in the 15 hr field). In this paper, we present new imaging of these LAEs from the Near Infrared Camera and Multi-Object Spectrometer (NICMOS; Thompson et al. 1998). These images, obtained through the J_{110} filter with the NIC2 camera, confirm the presence of the two LAEs in the 15 hr field. In Section 2, we present our observations and data reduction, as well as the process by which we match our spectroscopically discovered sources with NICMOS detections. In Section 3, we discuss the properties of these three LAEs and Section 4 contains a summary of our results. We use $H_0 = 70\,\mathrm{km\,s^{-1}\,Mpc^{-1}}$, $\Omega_\Lambda = 0.7$, $\Omega_M = 0.3$, and AB magnitudes throughout.

2. OBSERVATIONS AND DATA REDUCTION

2.1. NICMOS Imaging

Each of the three LAEs was observed for five orbits (13.4 ks) with the NICMOS 2 camera. The images were then processed in several steps to make final mosaics. First, images were corrected for the quadrant-dependent variable bias (the "pedestal effect"), and South Atlantic Anomaly darks were subtracted from impacted orbits. Next, we used the IRAF task *rnlincor* to correct the count-rate-dependent nonlinearity documented by de Jong (2006). With this approach, the zero point remained unchanged at $J_{110} = 23.69$. For our configuration of J_{110} with NICMOS 2, the nonlinearity correction was substantial and amounted to -0.25 mag for the $J_{110} = 23$–26 mag sources in our images. Following this correction, the images were sky subtracted, using the NICRED package (McLeod 1997). Then, the remaining vertical and horizontal bands in the images were removed by subtracting a model sky frame constructed by taking the median of each column and smoothing it by a three pixel wide boxcar. (This step was repeated for rows to remove any top to bottom banding or gradients.) After this, we identified bad pixels in the images following the procedures used by the Multidrizzle software (Koekemoer et al. 2002). A truth image was made by aligning the images and creating a median stack. This image was shifted back to the frame of the original input image, and pixels deviant by more than 3σ were flagged as bad pixels. Finally, images were combined with drizzle with bad pixels masked using parameters recommended in the Dither Handbook: pixfrac = 0.6 and scale = 0.5. The final output pixels are 0.″038.

The resulting point-spread function (PSF), measured from the two point sources in these images, has an FWHM of 0.″1. Sensitivity was measured by randomly placing 0.″6 diameter apertures in the image, rejecting those that fell on sources and fitting a Gaussian to the "counts-per-aperture" distribution, as described in Henry et al. (2009). We found a 5σ sensitivity of $J_{110} = 26.5$ in this aperture. Using the point sources in our images, we measured the aperture correction to be 0.08 mag, so the 5σ total sensitivity is $J_{110} = 26.4$ (for a point source). Finally, using a few common sources per image, the astrometric solutions to the NICMOS images were aligned with the COSMOS survey for the 10 hr field, and the Sloan Digital Sky Survey for the 15 hr field.

2.2. Identifying the LAEs in NICMOS Images

The spectroscopic search and confirmation data are presented in Martin et al. (2008), where a difference was discovered between the World Coordinate System (WCS) zero points of COSMOS and that of our data. Namely, the position of MSDM 80+3 in the COSMOS/Subaru narrowband imaging is nearly 1″ west of the position found by Martin et al. In light of this offset, we improved our technique for deriving coordinates, by mapping a WCS solution to images taken through our slitmask. We tested these solutions for both the COSMOS and 15 hr field, using dozens of objects (per field) that have continuum detections in our spectra. We found (1σ) position uncertainties of 0.″3–0.″5 along the slits and 1.″0 perpendicular to the slits. The latter uncertainty naturally arises in all blind spectroscopic searches, because sources are not necessarily centered in the slits. For the COSMOS field, the slits are oriented east–west, so these uncertainties correspond to R.A. and decl., respectively. For the 15 hr field, the slit position angle (P.A.) was $-45°$.

In Figure 1, we show the NICMOS J_{110} images at the positions of the three LAEs. No obvious source is detected at the position of MSDM 80+3, but sources are detected within the 1σ position error ellipse for MSDM 29.5+5 and just outside it for MSDM 71−5. Photometry is presented in Table 1. We used 0.″6 diameter apertures, centered on the positions of the sources shown in Figure 1 for MSDM 29.5+5 and MSDM 71−5, and at the position of the narrowband detection for MSDM 80+3 (see Figure 2). A point-source model was adopted for the aperture correction, as explained in Section 2.1. While more light will be missed from extended sources, this loss amounts to at most 0.1–0.3 mag (in addition to the point-source aperture correction), as nearly all $z \sim 6$ galaxies have half-light radii, $r_{\rm hl} < 0.''2$ (Bouwens et al. 2004; Ferguson et al. 2004). As we cannot accurately determine the amount of missed flux, we adopt the point-source aperture correction of 0.1 mag and note this systematic uncertainty.

In order to determine whether the sources are likely to be associated with the LAEs, we calculated the probability that the NICMOS detections in the 15 hr field are from foreground galaxies. To do this, we obtained the publicly available catalogs of the NICMOS Ultra-Deep Field (UDF[4]; Thompson et al. 2005). For consistency with our aperture

[4] http://archive.stsci.edu/prepds/udf/udf_hlsp.html

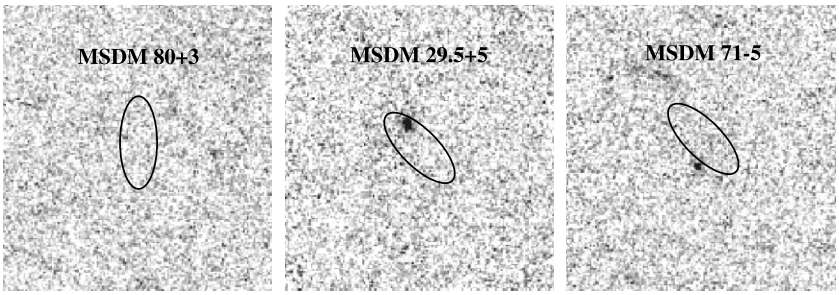

Figure 1. Postage stamp images of our NICMOS J_{110} observations of the three LAEs. The images are 6″ on a side with north up and east to the left. Ellipses mark the predicted positions of the LAEs, assuming that each fell at the center of the Magellan/IMACS spectroscopic slit. The sizes of the error ellipses are prescribed by the position uncertainties given in Section 2.2. Although MSDM 80+3 was detected in narrowband observations (Murayama et al. 2007), the position shown here is—as with the other two objects—the one determined from our IMACS spectroscopic observations. Measured positions of the J_{110} detections of MSDM 29.5+5 and MSDM 71−5 are given in Table 1.

Table 1
Rest-frame UV Properties

Name	R.A. (J2000)	Decl. (J2000)	J_{110} (AB)	F(Lyα) (10^{-18} erg s^{-1} cm^{-2})	W_0 (Å)	M_{UV} (AB)	SFR ($M_\odot$ yr^{-1})	r_{hl} (″)
MSDM 80+3	10 00 30.413	02 17 14.81	>26.9	28 ±4[a]	>146	>−19.8	<4.0	···
MSDM 29.5+5	15 22 57.900	−00 07 36.80	26.0 ± 0.1	18 ± 2	41 ± 6	−20.7	10	0.15
MSDM 71−5	15 24 08.920	−00 10 43.31	25.6 ± 0.1	22 ± 6	35 ±10	−21.1	14	0.14

Notes. J_{110} magnitudes are total, and equivalent width is given in the rest frame. Limits are 3σ, total, for a point source. As discussed in Section 3.1, the limit on MSDM 80+3 will be weaker if it is significantly extended. Coordinates given are measured from direct images of the sources: NICMOS for MSDM 29.5+5 and MSDM 71−5, and Subaru NB816 for MSDM 80+3. SFRs are estimated from the Madau et al. (1998) conversion, but will be higher if extinction is large or the galaxies are extremely young.
[a] Taken from the narrowband imaging measurement (Murayama et al. 2007).

photometry of the LAEs, we used 0.″6 diameter apertures. To $J_{110} = 26.1$, which is the aperture magnitude of the fainter of the two detected sources, we found cumulative number counts of ∼60 arcmin^{-2}. Therefore, there is less than a 1% chance of a foreground interloper falling within our positional error ellipse. For the brighter source, this probability is about 50% lower. We conclude with greater than 99% confidence that each of the NICMOS-detected sources is indeed an LAE discovered by Martin et al. (2008).

2.3. Lyα Contribution to Broadband Photometry?

Strong Lyα emission can, in some cases, contribute appreciably to broadband flux density (Schaerer & de Barros 2010), and for our objects this could happen. At $z = 5.7$, Lyα is included in the wide J_{110} bandpass, which covers approximately 8000 Å to 1.4 μm. However, the contribution is negligible for our objects—our measured Lyα fluxes account for only 5%–10% of the J_{110} flux densities for the two detected sources. This enhancement lies within our uncertainties, so no corrections are made to our photometry and equivalent width measurements.

3. DISCUSSION

3.1. MSDM 80+3: Comparison to Narrowband Observations

These NICMOS observations provide the first direct images of two sources (MSDM 29.5+5 and MSDM 71−5) which had previously only been detected in our spectroscopic data. On the other hand, the source which is undetected in J_{110}, MSDM 80+3, shows a strong detection in Subaru narrowband imaging with the NB816 filter (object 55 in Murayama et al. 2007). In Figure 2, we show the narrowband image of MSDM 80+3, with our position error ellipse overlaid. Our improved coordinates for MSDM 80+3 are roughly consistent with the NB816 source in Murayama et al. The newly derived position is 0.″7 west

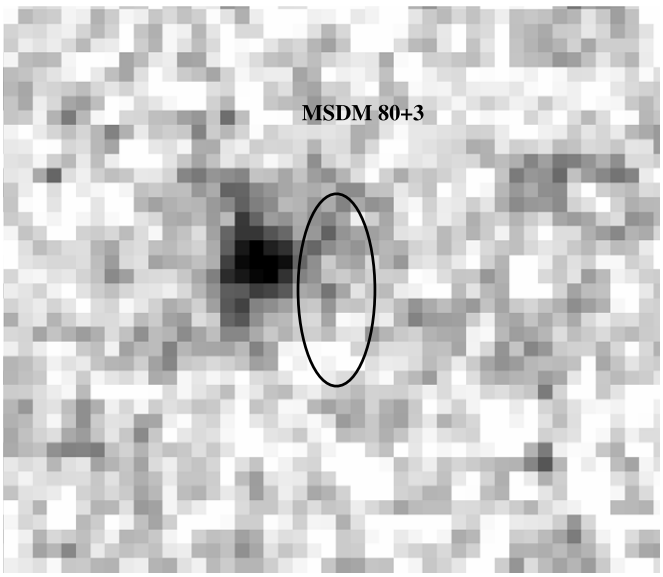

Figure 2. NB816 image of MSDM 80+3, 6″ on a side with north up and east to the left. The ellipse marks the predicted position, at the center of the slit, with its size prescribed by the position uncertainties described in Section 2.2. In this image, our IMACS slit is located left to right. The image shown here is the original resolution (0.″7 seeing), rather than the PSF-matched image used for photometry.

of the NB816 detection, while the previous position given in Martin et al. was 1″ east. This position offset along the slit is still large compared to other sources, including those discussed in Section 2.2 and for 52 lower redshift line emitters that are in common between Martin et al. and the COSMOS NB816 sample. Given the slight offset perpendicular to the slit (0.″4) shown in Figure 2, one possibility is that the Lyα emission from this object is extended, and our slit subtended an outlying region of the galaxy. Some evidence for this hypothesis is present in

the Subaru narrowband image (Figure 2), where MSDM 80+3 is marginally resolved.

The absence of continuum emission could indicate that the source is extended in the continuum, although extended Lyα emission need not imply a similarly extended stellar continuum. The upper bound of i-dropout LBG sizes is $r_{\rm hl} < 0\farcs2$ (in the rest-frame UV; Bouwens et al. 2004), which corresponds to 5.3 pixels in our drizzled NIC2 images. Using the IRAF artdata package, we verified that a galaxy of this size would be undetected in our NICMOS data at $J_{110} > 26.5$. It is tempting to conclude from the low-surface brightness signal at the position of MSDM 80+3 in our NICMOS image that it may be more extended in the rest-frame UV. However, this LAE fell on the bad central column[5] in these observations, and similar artifacts appear at other locations along the column. The weight maps produced by drizzle indicate that noise is ∼30% higher at these locations relative to the rest of the image, so the extended feature is not significant. Nevertheless, the J_{110} non-detection could imply that MSDM 80+3 is more extended in the continuum than the other two LAEs (MSDM 29.5+5 and 71−5), which have half-light radii (measured with SExtractor) of $0\farcs15$ and $0\farcs14$.

The hypothesis that the Lyα emission may be extended is also supported by our line flux measurement, which is a factor of 2 lower than the Subaru NB816 imaged line flux. This difference is larger than is expected for a point source, unless the object fell on the edge of our $1\farcs5$-wide slit. As noted above, in the narrowband image coordinates, MSDM 80+3 is $0\farcs4$ north of the slit center. Using the point-source slit loss models from Martin et al. (2008) at this position, we expect only about a 20% slit loss. The effect of the non-uniform response of the NB816 filter on SuprimeCam is negligible for MSDM 80+3, because our measured wavelength is near the central wavelength of the NB816 transmission. Furthermore, lines at wavelengths away from the center of the NB816 bandpass would have decreased the observed Lyα flux relative to our spectroscopic measurement—the opposite of what we observe. Generally, sources found through blind spectroscopy do not fall at the center of the slit; for larger samples the impact of slit losses on the LF is modeled statistically.

3.2. Properties

Equivalent widths, UV luminosities, and UV-continuum-derived SFRs are given in Table 1. We assume a flat UV spectrum ($f_\lambda \propto \lambda^{-2}$), consistent with observations of LAEs with Lyα luminosities and redshifts similar to those of our objects (Pirzkal et al. 2007) and with $z \sim 6$ LBGs in the NICMOS UDF (Stanway et al. 2005; Bouwens et al. 2009). Therefore, although the center of the J_{110} filter corresponds to ∼1700 Å in the rest frame, our best estimate is that k-corrections are negligible. We note that $M^*_{\rm UV} = -20.2$ at $z \sim 6$ (Bouwens et al. 2007), so the UV luminosities that we measure are consistent with typical sources observed at this redshift—within a factor of 2 of L^* for the two J_{110}-detected sources.

SFRs are derived using the 1500 Å conversion from Madau et al. (1998). UV-continuum-based estimates of SFRs are thought to be more reliable than those from Lyα; nevertheless, these continuum-based estimates come with several caveats. First, the conversion is valid only when the characteristic stellar age is older than the main-sequence lifetime of O- and B-stars. At young ages ($\lesssim$20 Myr), the true SFR may be a few times larger. Second, we have not corrected the UV luminosities for dust extinction, so again the SFRs given in Table 1 may be underestimated. However, in general, $z \sim 6$ galaxies are not thought to be very dusty (Bouwens et al. 2009), so dust corrections to our SFRs need not be very large. Third, uncertainties in the initial mass function (IMF) slope and mass cutoffs may be just as important, as they can change the SFR by a factor of a few (Henry et al. 2009). On the other hand, the two-photon nebular continuum is not expected to make a significant contribution to the UV luminosity, since it is generally dwarfed by the stellar contribution. While some sources are purported to have spectra dominated by the two-photon continuum, such objects appear to be rare (Fosbury et al. 2003; Raiter et al. 2010) and are predicted to have rest-frame Lyα equivalent widths $\gtrsim$1000 Å (Schaerer 2002, with coefficients from Aller 1984).

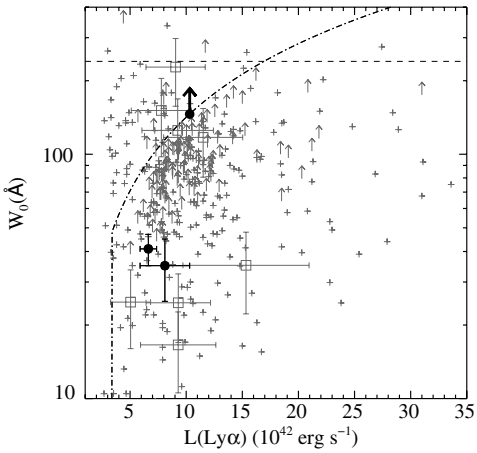

Figure 3. Rest-frame equivalent widths of the sources in our survey (black) fall in the normal range established by other various Lyα searches at $z = 4$–6 (gray). These include sources discovered with the Advanced Camera for Survey grism (squares; Pirzkal et al. 2007) and narrowband imaging surveys (Hu et al. 2004; Shimasaku et al. 2006; Murayama et al. 2007; Ouchi et al. 2009; Wang et al. 2009). The dot-dashed line shows the maximum detectable equivalent width when $M_{\rm UV} = -19.8$ is reached, as is the case with our NICMOS observations. The dashed horizontal line marks $W_0 = 240$ Å, which is often quoted as the maximum equivalent width seen in "normal" stellar populations (Charlot & Fall 1993; Malhotra & Rhoads 2004). It is important to note that the equivalent width uncertainties typically exceed 100 Å when W_0 is large, so the sources above this line should be viewed with caution.

The equivalent widths that we measure are consistent with those of LAEs at high redshift, as shown in Figure 3. We do not make any correction for IGM absorption on the Lyα emission, as has been done for some objects at $z \sim 6$ (e.g., Shimasaku et al. 2006). While it is possible that the Lyα emission emergent from the galaxy is larger than observed, the amount of attenuation is uncertain because the resonant scattering of Lyα photons shifts the emission toward redder wavelengths (Verhamme et al. 2008). It is not surprising that we do not observe any sources that are both UV luminous and have high-equivalent widths. As Nilsson et al. (2009) point out, this may be a consequence of both classes of objects being rare rather than a correlation of equivalent width with UV luminosity as has been suggested by Ando et al. (2006).

The three LAEs that we present are consistent with the range of equivalent widths that are easily explained by "normal" stellar populations, with ages older than 10 Myr and a Salpeter IMF. However, deeper continuum observations of MSDM 80+3 could prove that its equivalent width is much larger. There are several different models that can explain very large equivalent widths. First, extremely young ages and/or top-heavy IMFs can result in $W_0 > 240$ Å (e.g., Malhotra & Rhoads 2004). Second, a

[5] http://www.stsci.edu/hst/nicmos/performance/anomalies

multi-phase interstellar medium has sometimes been invoked to preferentially absorb UV-continuum photons (Neufeld 1991; Hansen & Oh 2006; Scarlata et al. 2009; Finkelstein et al. 2009). Third, gravitational cooling radiation in the absence of star formation is predicted to result in $W_0 > 1000$ Å (Dijkstra 2009). However, such high-equivalent width objects are probably rare, as only a few sources in Figure 3 lie at $W_0 > 240$ Å. It is important to note that the uncertainty on such high-equivalent width sources typically exceeds 100 Å because of weak continuum detections, so these measurements should be viewed with caution.

It is interesting to consider whether the LAEs in our survey would be selected as *i*-dropout LBGs at $z \sim 6$, because the connection between the two populations is currently unclear. While it is generally understood that LAEs can be missed by LBG searches when their continuum is too faint, the selection of brighter sources can also be influenced by strong line emission (e.g., Stanway et al. 2007, 2008). At $z \leqslant 5.7$, Lyα falls in the *i* band, and galaxies can sometimes be too blue in i–z to be included in *i*-dropout samples, even when an identical galaxy without Lyα emission would be included in such a sample. (It is worth noting that such objects could be included in $z \sim 5$ *R*-dropout samples, provided that the i–z color is not too red.) Strong Lyα emission may influence the color selection of all three galaxies presented here. Assuming a flat UV slope ($f_\lambda \propto \lambda^{-2}$), we estimate i–$z = 1.2$ and 1.3 for MSDM 29.5 and MSDM 71−5, near the i–$z = 1.3$ cut used by most LBG studies (e.g., Bouwens et al. 2007). The inclusion of sources such as these would depend on photometric scatter and the true value of the UV slope. On the other hand, MSDM 80+3, which is undetected in the J_{110} images, would be unlikely to be included in *i*-dropout samples. The Lyα flux contributes substantially to the *i* band, so even in the absence of any continuum we would expect $i = 27.6$. Assuming $z_{850} > 26.9$—as inferred from our J_{110} limit—implies that we would expect i–$z \leqslant 0.7$. Therefore, even if MSDM 80+3 could be detected in very deep imaging such as the UDF, it would be too much blue to be included in the *i*-dropout samples. This exercise emphasizes the importance of including Lyα emission in the modeling of LBG selection functions, as is done by Bouwens et al. (2007).

4. CONCLUSIONS

Spectroscopic searches for high-redshift emission-line galaxies have now been shown as a viable technique for improving sensitivity to faint emission-line galaxies (Santos et al. 2004; Sawicki et al. 2008; Lemaux et al. 2009). In particular, Martin et al. (2008) have successfully identified three $z = 5.7$ LAEs with multislit narrowband spectroscopy. We have presented NICMOS observations of these three LAEs, obtained with the high spatial resolution NIC2 camera. These images confirm the two sources which had only previously been seen in our IMACS spectroscopic observations. Furthermore, the J_{110} data provide some constraints on the properties of these galaxies. We find that the UV luminosities, SFRs, equivalent widths, and sizes are all consistent with a redshift of $z = 5.7$. The two detected sources have $L_{\rm UV}$ within a factor of 2 of $L^*_{\rm UV}$ (as measured by Bouwens et al. 2007), and equivalent widths are well within the range of values seen at all redshifts. In addition, the non-detection of MSDM 80+3, in combination with a substantial slit loss of Lyα flux, suggests that the source may be somewhat extended.

These new observations further prove the success of multislit narrowband spectroscopy as a means to uncover faint, high-redshift emission-line galaxies. Further efforts for extending this technique to much fainter LAEs are already underway (A. Dressler et al. 2010, in preparation). Longer exposures with the recently upgraded IMACS detectors can reach Lyα luminosities at $z \sim 6$ that have previously only been realized in gravitational lensing surveys along the critical lines of galaxy clusters (e.g., Santos et al. 2004). At the limit of our new survey (at least 4×10^{-18} erg s^{-1}cm^{-2}), rest-frame equivalent widths above 150 Å would imply a *z*-band magnitude fainter than 29—a regime that is currently only accessible from the small area covered by the UDF and UDF Parallels. These new blind spectroscopic observations will provide an ideal sample of low-luminosity $z = 5.7$ LAEs that will be detectable with NIRCAM, NIRSPEC, and the Tunable Filter Imager on the *James Webb Space Telescope* in modest exposure times ($\lesssim$10,000 s). Such future observations will provide critical insight into the building blocks of galaxies by measuring their stellar and nebular (line+continuum) emission.

This work is supported by *HST* GO-11183. We thank Matt Auger, Peter Capak, and Kristian Finlator for helpful suggestions and discussions. We are grateful to the anonymous referee for comments that improved this manuscript.

REFERENCES

Ajiki, M., et al. 2004, PASJ, 56, 597
Aller, L. H. 1984, Physics of Thermal Gaseous Nebulae (Astrophys. Space Sci. Lib. 112; Dordrecht: Reidel)
Ando, M., Ohta, K., Iwata, I., Akiyama, M., Aoki, K., & Tamura, N. 2006, ApJ, 645, L9
Bouwens, R. J., Illingworth, G. D., Blakeslee, J. P., Broadhurst, T. J., & Franx, M. 2004, ApJ, 611, L1
Bouwens, R. J., Illingworth, G. D., Franx, M., & Ford, H. 2007, ApJ, 670, 928
Bouwens, R. J., Illingworth, G. D., Franx, M., & Ford, H. 2008, ApJ, 686, 230
Bouwens, R. J., et al. 2009, ApJ, 705, 936
Bouwens, R. J., et al. 2010, ApJ, 709, L133
Bunker, A. J., et al. 2009, arXiv:0909.2255
Charlot, S., & Fall, S. M. 1993, ApJ, 415, 580
Dawson, S., Rhoads, J., Malhotra, S., Stern, D., Wang, J., Dey, A., Spinrad, H., & Jannuzi, B. 2007, ApJ, 671, 122
de Jong, R. S. 2006, NICMOS Instrum. Sci. Rep. 2006-003 (Baltimore, MD: STScI)
Dijkstra, M. 2009, ApJ, 690, 82
Dijkstra, M., Wyithe, J. S. B., & Haiman, Z. 2007, MNRAS, 379, 259
Dow-Hygelund, C. C., et al. 2007, ApJ, 660, 47
Dressler, A., et al. 2006, Proc. SPIE, 6269, 13
Dunkley, J., et al. 2009, ApJS, 180, 306
Eyles, L. P., Bunker, A. J., Ellis, R. S., Lacy, M., Stanway, E. R., Stark, D. P., & Chiu, K. 2007, MNRAS, 374, 910
Eyles, L. P., Bunker, A. J., Stanway, E. R., Lacy, M., Ellis, R. S., & Doherty, M. 2005, MNRAS, 364, 443
Fan, X., Carilli, C. L., & Keating, B. 2006, ARA&A, 44, 415
Ferguson, H. C., et al. 2004, ApJ, 600, L107
Finkelstein, S. L., Rhoads, J. E., Malhotra, S., & Grogin, N. 2009, ApJ, 694, 465
Finkelstein, S. L., Rhoads, J. E., Malhotra, S., Grogin, N., & Wang, J. 2008, ApJ, 678, 655
Finkelstein, S. L., Rhoads, J. E., Malhotra, S., Pirzkal, N., & Wang, J. 2007, ApJ, 660, 1023
Fosbury, R. A. E., et al. 2003, ApJ, 596, 797
Fruchter, A., & Hook, R. N. 1997, Proc. SPIE, 3164, 120
Furlanetto, S. R., Zaldarriaga, M., & Hernquist, L. 2006, MNRAS, 365, 1012
Gawiser, E., et al. 2006, ApJ, 642, L13
Gawiser, E., et al. 2007, ApJ, 671, 278
Gronwall, C., et al. 2007, ApJ, 667, 79
Haiman, Z., & Cen, R. 2005, ApJ, 623, 627
Hansen, M., & Oh, P. S. 2006, MNRAS, 367, 979
Henry, A. L., et al. 2009, ApJ, 697, 1128
Hu, E., et al. 2002, ApJ, 568, L75
Hu, E., et al. 2004, AJ, 127, 563

Kashikawa, N., et al. 2006, ApJ, 648, 7
Koekemoer, A. M., Fruchter, A. S., Hook, R. N., & Hack, W. 2002, in *HST* Calibration Workshop, ed. S. Arribas, A. M. Koekemoer, & B. Whitmore (Baltimore, MD: STScI), 337
Kornei, K. A., Shapley, A. E., Erb, D. K., Steidel, C. C., Reddy, N. A., Pettini, M., & Bogosavljević, M. 2010, ApJ, 711, 693
Lai, K., et al. 2008, ApJ, 674, L70
Lemaux, B. C., et al. 2009, ApJ, 700, 20
Madau, P., Pozetti, L., & Dickinson, M. 1998, ApJ, 498, 106
Malhotra, S., & Rhoads, J. E. 2002, ApJ, 565, L71
Malhotra, S., & Rhoads, J. E. 2004, ApJ, 617, L5
Martin, C. L., & Sawicki, M. 2004, ApJ, 603, 414
Martin, C. L., Sawicki, M., Dressler, A., & McCarthy, P. 2008, ApJ, 679, 942
Marzke, R. O., et al. 1999, in ASP Conf. Ser. 191, in Photometric Redshifts and the Detection of High Redshift Galaxies, ed. R. Weymann et al. (San Francisco, CA: ASP), 148
McLeod, B. A. 1997, in The 1997 *HST* Calibration Workshop with a New Generation of Instruments, NICRED: Reduction of NICMOS MULTIACCUM Data with IRAF, ed. S. Casertano et al. (Baltimore, MD: STScI), 281
McLure, R. J., Cirasuolo, M., Dunlop, J. S., Foucaud, S., & Almaini, O. 2009, MNRAS, 395, 2196
McQuinn, M., Hernquist, L., Zaldarriaga, M., & Dutta, S. 2007, MNRAS, 381, 75
Meier, D. L. 1976, ApJ, 203, L103
Murayama, T., et al. 2007, ApJS, 172, 523
Neufeld, D. A. 1991, ApJ, 370, L85
Nilsson, K. K., Möller-Nilsson, O., Møller, P., Fynbo, J. P. U., & Shapley, A. E. 2009, MNRAS, 400, 232
Nilsson, K. K., Møller, P., Möller, O., Michałowski, M. J., Watson, D., Ledoux, C., Rosati, P., Pedersen, K., & Grove, L. F. 2007, A&A, 471, 71
Ouchi, M., et al. 2008, ApJS, 176, 301
Ouchi, M., et al. 2009, ApJ, 696, 1164
Pirzkal, N., Malhotra, S., Rhoads, J. E., & Xu, C. 2007, ApJ, 667, 49
Raiter, A., Fosbury, R. A. E., & Teimoorinia, H. 2010, A&A, 510, 109
Rauch, M. R., et al. 2008, ApJ, 681, 586
Rhoads, J., et al. 2004, ApJ, 611, 59
Ryan-Weber, E. V., Pettini, M., Madau, P., & Zych, B. J. 2009, MNRAS, 395, 1476
Santos, M. R. 2004, MNRAS, 349, 1137
Santos, M. R., Ellis, R. S., Kneib, J.-P., Richard, J., & Kuijken, K. 2004, ApJ, 606, 683
Sawicki, M., et al. 2008, ApJ, 687, 884
Scarlata, C., et al. 2009, ApJ, 704, L98
Schaerer, D. 2002, A&A, 382, 28
Schaerer, D., & de Barros, S. 2010, A&A, 515, 73
Scoville, N., et al. 2007, ApJS, 172, 1
Shapley, A. E., Steidel, C. C., Pettini, M., & Adelberger, K. L. 2003, ApJ, 588, 65
Shimasaku, K., et al. 2006, PASJ, 58, 313
Simcoe, R. 2006, ApJ, 653, 977
Stanway, E. R., Bremer, M. N., & Lehnert, M. D. 2008, MNRAS, 385, 493
Stanway, E. R., McMahon, R. G., & Bunker, A. J. 2005, MNRAS, 359, 1184
Stanway, E. R., et al. 2007, MNRAS, 376, 727
Stark, D. P., Ellis, R. S., Chiu, K., Ouchi, M., & Bunker, A. 2010, arXiv:1003.5244
Stark, D. P., Ellis, R. S., Richard, J., Kneib, J.-P., Smith, G. P., & Santos, M. R. 2007, ApJ, 663, 10
Steidel, C. C., Giavalisco, M., Pettini, M., Dickinson, M., & Adelberger, K. L. 1996, ApJ, 462, L17
Taniguchi, Y., et al. 2009, ApJ, 701, 915
Thompson, R. I., Reike, M., Schneider, G., Hines, D. C., & Corbin, M. R. 1998, ApJ, 492, L95
Thompson, R. I., et al. 2005, AJ, 130, 1
Tran, K.-V. H., Lilly, S. J., Crampton, D., & Brodwin, M. 2004, ApJ, 612, L89
Vanzella, E., et al. 2009, ApJ, 695, 1163
Verhamme, A., Schaerer, D., Atek, H., & Tapken, C. 2008, A&A, 491, 89
Wang, J.-X., Maholtra, S., Rhoads, J. E., Zhang, H.-T., & Finkelstein, S. 2009, ApJ, 706, 762
Westra, E., et al. 2006, A&A, 455, 61
Yan, H., Dickinson, M., Giavalisco, M., Stern, D., Eisenhardt, P. R. M., & Ferguson, H. C. 2006, ApJ, 651, 24